Journal of Biomedical Materials Research Part B: Applied Biomaterials

WILEY

Society For Biomaterials

RESEARCH ARTICLE OPEN ACCESS

Microscopic Acid-Induced Degradation and Elemental Release From Thermoformed and 3D-Printed Orthodontic Aligners in a Simulated Gastric Environment

Piero Antonio Zecca[1] | Eleonora Ivonne Scurati[1] | Francesca Zara[2,3] | Mario Raspanti[1] | Niccolò Baranzini[4] | Gilberto Binda[5,6] | Marco Serafin[7] | Alberto Caprioglio[2,3] | Marina Borgese[1]

[1]Department of Medical Innovation and Technology, University of Insubria, Varese, Italy | [2]Department of Biomedical, Surgical and Dental Sciences, University of Milan, Milan, Italy | [3]Fondazione IRCCS Cà Granda, Ospedale Maggiore Policlinico, Milan, Italy | [4]Department of Biotechnology and Life Sciences, University of Insubria, Varese, Italy | [5]Department of Science and High Technology, University of Insubria, Como, Italy | [6]Norwegian Institute for Water Research, Oslo, Norway | [7]Department of Biomedical Sciences for Health, University of Milan, Milan, Italy

Correspondence: Marco Serafin (marco.serafin@unimi.it)

Received: 2 July 2025 | **Revised:** 19 August 2025 | **Accepted:** 9 September 2025

Funding: The authors received no specific funding for this work.

Keywords: 3D printing | acid degradation | clear aligners | microscopy | orthodontics | plastic release | thermoforming

ABSTRACT

Clear aligners have revolutionized orthodontic treatment, yet concerns are rising about microplastics (MPs) and nanoplastics (NPs) released from these devices through mechanical wear and chemical degradation. Once ingested, these particles may undergo structural and chemical transformations in the gastrointestinal tract, particularly under acidic gastric conditions. Despite growing environmental and toxicological awareness, the degradation patterns of aligner materials remain largely unexplored. This study evaluated the acid-induced degradation and elemental release of thermoformed (TFA) and direct-printed (DPA) aligners in a simulated gastric environment. TFA (Invisalign SmartTrack) and DPA (Graphy TC-85DAC) samples were exposed to hydrochloric acid (pH 2). Surface acid-induced degradation was monitored using atomic force microscopy (AFM) over 60 min, while elemental release was quantified using inductively coupled plasma mass spectrometry (ICP-MS) following acid digestion on 0.5 M HCl leachates after 7 days. TFA rapidly disintegrated into an amorphous gel, preventing AFM imaging at pH 2. DPA maintained integrity and showed progressive roughening: RMS roughness rose from 10.06 to 10.97 nm (+9%; $p < 0.001$), mean roughness from 7.85 to 8.49 nm (+8%; $p = 0.002$), and maximum height from 68.31 to 76.51 nm (+12%; $p = 0.038$). ICP-MS of digested matrices revealed distinct elemental fingerprints: TFA was dominated by Sn (33.42 mg/kg), K (21.35 mg/kg), and Na (13.34 mg/kg); DPA by Ca (36.63 mg/kg), Na (11.87 mg/kg), and Fe (3.2 mg/kg). In 7-day 0.5 M HCl leachates, TFA released Sb 0.13 and Sn 0.09 mg/kg, whereas DPA showed Sb 0.03 and Sn 0.11 mg/kg; DPA leachates were richer in Ca (7.57 mg/kg) and Fe (1.57 mg/kg). DPA exhibited quantifiably slower acid erosion than TFA and distinct elemental release profiles at longer extraction, supporting greater acid-phase stability of DPA and providing elemental markers to trace aligner-derived particles. The results pertain to Invisalign SmartTrack and Graphy TC-85DAC and should not be generalized to all thermoformed or 3D-printed aligners. These findings emphasize the need for biostable, environmentally safer materials in orthodontics, especially considering the ingestion and systemic distribution of MPs.

1 | Introduction

Clear aligners are widely used in orthodontics due to their aesthetic advantages and growing demand. With advancements in material science, the main manufacturing techniques are thermoforming and, nowadays, direct 3D printing [1]. Thermoformed aligners (TFA) and direct printed aligners (DPA) offer distinct mechanical properties and benefits. However, their stability and biocompatibility, when subjected to mechanical stress, remain critical areas of inquiry.

In recent years, research has highlighted the potential release of microplastics (MPs) and nanoplastics (NPs) by orthodontic appliances, especially in response to wear, environmental exposure, and chemical interactions [2]. Thermoplastic materials such as PET-G and polyurethanes, commonly used in thermoformed aligners, are designed to be biocompatible and durable under typical intraoral conditions. However, they are still susceptible to structural degradation and potential ingestion [3]. Due to that, prolonged exposure to acidic and enzymatic environments, as would occur if aligner MPs or degraded particles enter the gastrointestinal tract, could accelerate the subsequent plastic release and both chemical and physical transformations [4].

On the other hand, DPA is produced using photopolymerization-based techniques where UV-curable resins form aligners. Unlike thermoforming, these methods offer greater accuracy and material efficiency [5]. The degree of conversion of photopolymers, influenced by layer thickness, light exposure, and post-curing, affects mechanical properties and biocompatibility [6]. Incomplete polymerization can lead to residual monomer release, which may be exacerbated under acidic oral conditions, potentially impacting cytotoxicity and material integrity [7].

The ingestion of MPs and NPs from everyday products has become a growing concern in medical and environmental research [8]. Preliminary studies suggest that TFAs and DPAs produce MPs and NPs under specific environmental stresses, raising concerns about their potential effects on the digestive tract [2, 9–11]. In fact, once in the gastrointestinal tract, MPs could be broken down further into NPs and transformed components due to the stomach's acidic environment, potentially enabling them to permeate biological membranes. This breakdown, facilitated by gastric acids and enzymes, could allow these particles to infiltrate cells and tissues and possibly cross biological barriers, posing unknown risks to human health [12]. In addition, the acidic conditions of the gastrointestinal tract can induce the release of potentially toxic plastic additives [13].

Therefore, the present study evaluated the material response of TFA and DPA in a simulated acidic gastric environment, focusing on their structural acid-induced degradation and the release of elemental components under acidic conditions.

2 | Materials and Methods

This study examined two types of orthodontic aligners: TFA and DPA, both tested in a simulated gastric environment. TFA samples comprised Invisalign SmartTrack aligners (Align Technology Inc., Tempe, AZ, USA), a proprietary multilayer aromatic thermoplastic polyurethane and copolyester blend. DPA samples were produced by Graphy Tera Harz TC-85DAC resin (Graphy Inc., Seoul, South Korea) with SprintRay PRO 95 3D printer (SprintRay Europe GmbH, Weiterstadt, Germany) following the manufacturer's specifications, with post-curing completed via a Tera Harz Cure THC2 device (Graphy Inc.). TC-85DAC is a patented biocompatible shape-memory resin composed primarily of urethane acrylate oligomers and photoinitiators.

2.1 | Atomic Force Microscopy (AFM) Surface Analysis

AFM analysis was used for surface topography with nanometric resolution. Samples measuring 5×5×0.6 mm (nominal thickness) from each aligner type were prepared and mounted on a delaminated mica disc to prevent contamination. A hydrochloric acid (0.01 M HCl) solution at pH 2 was prepared to simulate the stomach's acidic environment, a value within the fasted gastric pH range, and aligned with gastric residence half-times reported for small particles [14]. Each sample was subsequently immersed in 200 μl of HCl solution on the AFM stage, and imaging began immediately in immersion mode. AFM analysis was conducted using a Digital Instruments Nanoscope IIIa (Santa Barbara, CA, USA), with a scan size of 1×1 mm, a resolution of 512 lines per frame, and a scan rate of 1.968 Hz. AFM was operated in tapping mode to prevent damage to the samples. The Z-axis sensitivity was calibrated to 8.40 nm/V, and the piezo calibration was set at 440 V.

Images were acquired at 6 min time points over a total period of 1 h. Every 15 min into the observation period, an additional HCl solution was added to compensate for evaporation and maintain consistent acidity levels. The same region of interest (ROI) was used across all scans for consistent spatial analysis of surface changes over time. The images were then processed using Fiji 1.54 software, while AFM scan data analysis was performed with Gwyddion software (Department of Nanometrology, Czech Metrology Institute, Czech Republic).

AFM surface analysis was performed on a single sample and comprised the quantification of the following parameters, registered before the acidic treatment (T0) and after the complete cycle of induced degradation (T10):

- Average value: the mean surface height measured relative to a reference plane for roughness quantification.
- RMS roughness (Sq): root-mean-square roughness, representing the standard deviation of surface heights.
- Mean roughness (Sa): the arithmetic mean of the absolute surface height deviations from the reference plane
- Excess kurtosis: indicates the sharpness of surface height distribution relative to a normal distribution.
- Maximum: highest surface height measured from the reference plane.
- Median: median surface height measured from the reference plane

- Minimum: lowest surface height measured from the reference plane.
- Maximum peak height (Sp): the height of the highest peak measured from the reference plane.
- Maximum pit depth (Sv): the depth of the deepest valley measured from the reference plane.
- Maximum height (Sz): vertical distance between the highest peak and deepest valley.

Also, a time-lapse photo was generated by sequentially overlaying the images captured at different time points, providing a dynamic visualization of the surface changes over time. Baseline AFM comparison between TFA and DPA untreated samples was already reported by a previous study [2]. In the present protocol, pre-exposure AFM was avoided, focusing instead on a one-shot, time-lapse AFM under a pH 2 HCl solution.

Statistical analysis involved linear regression to evaluate changes in AFM-measured surface parameters over time. Measurements taken at multiple intervals from the same sample were used to assess whether observed variations were statistically significant, indicating genuine morphological changes rather than random fluctuations. A *p*-value less than 0.05 was considered statistically significant.

2.2 | Inductively Coupled Plasma–Mass Spectrometry (ICP-MS) for Elemental Release Analysis

Following AFM imaging, spectroscopic analysis was performed to detect potentially dissolved atoms from the aligner materials. The elemental content of aligners was obtained by acid digestion, followed by ICP-MS using a recently developed method for the digestion of plastic polymers [15]. Moreover, an accelerated extraction was consistent with stringent screening approaches for plastic leachables and complements shorter pH 2 incubations used in recent ICP-MS studies of polymeric materials [16].

The total metal content in the aligners was determined after acid digestion. This process was obtained through an ETHOS One microwave system (Milestone Srl, Sorisole, Italy) equipped with 10 polytetrafluoroethylene (PTFE) vessels. Samples of each material were first cut using ceramic scissors into pieces of ca. 5 mm. Then, approximately 50 mg of the sample was weighed and inserted into each vessel, along with 4 mL of HNO_3 and 1 mL of H_2SO_4. The materials were then digested by applying a temperature ramp reaching 200°C for 45 min, consisting of a 30-min heating and a 15-min holding time. Afterwards, further digestion at room temperature was performed: 0.1 mL of H_2O_2 was added to each vessel, and, following gentle stirring, the reaction was allowed to continue for 30 min at room temperature, after which another 0.1 mL of H_2O_2 addition was made. The vessels were left to cool to room temperature; then, solutions were transferred to pre-cleaned low-density polyethene (LDPE) bottles and diluted to 20 g with Milli-Q ultrapure water bath (Merck-Millipore, Burlington, MA, USA).

In addition, the leaching of metals from the aligners was simulated using a 0.5 mol/L HCl solution. To do so, about 500 mg of aligner fragments were weighed and put in 30 mL LDPE bottles. Then, 20 mL of HCl was added to the bottles. The bottles were then closed and put in an orbital shaker at 150 rpm at room temperature, and the solution was finally collected after 7 days.

TABLE 1 | Working parameters of ICP-MS.

Parameter	Value
RF Power	1550 W
Nebulizer gas flow	1.06 L/min
Auxiliary gas flow	0.80 L/min
Cooling gas flow	13.99 L/min
Dwell time	300 ms
Flow rate (collision cell)	4.34 mL/min
Sampling depth	5 mm

All solutions (both after acid-induced degradation and leaching in 0.5 mol/L HCl) were then filtered using 0.45 μm nylon filters, diluted, and spiked with two internal standards (Rh and Re, respectively). These solutions were then analyzed using an ICAP Q ICP-MS (Thermo Scientific, Waltham, MA, USA); working parameters are reported in Table 1.

External calibration was employed for element quantification. The analyzed elements were Na, Mg, Al, K, Ca, Ti, Cr, Mn, Fe, Cu, Sr, Sn, Sb, As, Cd, Cr, Pb, Sb, Sn, and Zn.

Method precision was assessed by analyzing 3 digestion and extraction replicates and computed as relative standard deviation (RSD) as in the following equation:

$$Sigma\frac{\sigma}{\mu}\%$$

where σ is the standard deviation, and μ is the average of the three replicate measures. The limit of detection (LOD) was obtained after the analysis of 5 procedural blank samples (i.e., acid solutions underwent digestion and dilution without the addition of the sample for the digestions and HCl solutions without the addition of aligners for the extractions) and was calculated as 3 times the SDs of the blanks [17].

3 | Results

3.1 | AFM Surface Analysis

The TFA sample demonstrated pronounced susceptibility to acidic environments, with rapid surface roughening observed upon immersion in HCl at pH 2. The material's structural integrity was compromised by forming a gel-like amorphous mass, even after repeated tests. This phenomenon rendered AFM imaging impossible due to the inability to acquire data; therefore, only DPA samples could acquire AFM images.

The DPA sample resisted acid-induced degradation better than the TFA one. AFM was employed to investigate the

morphological degradation of microplastics during 1 h of continuous immersion in HCl. Surface roughening occurred more slowly, allowing AFM imaging and subsequent quantification of surface parameters, as shown in Table 2.

Analysis of RMS roughness (Sq) and mean roughness (Sa) further supports the hypothesis of surface roughening. Both parameters exhibited a significant increase. This suggests that the acid treatment effectively eroded the material, creating a more irregular topography due to acid exposure. This phenomenon was also confirmed by a reduction in excess kurtosis. However, the excess kurtosis values showed a slight decrease, even non-statistically significant, implying that while the surface became rougher, the distribution of surface features remained relatively uniform at the end of the exposure, without a corresponding rise in sharp or isolated peaks. Interestingly, kurtosis's values exhibited huge variability, indicating a dynamic change in surface morphology. This combination suggests that HCl etching induces a broader and more homogeneous roughening effect rather than creating localized, extreme surface irregularities.

Data showed a consistent increase in surface elevation metrics, but surface degradation was expected to manifest as material loss under the assumption that acid exposure cannot generate new topographic peaks. Based on this, the maximum peak height (Sp) was used as a reference, and other parameters were tracked relative to it.

Therefore, the observed statistically significant increase in maximum peak height (Sp) indicated that, as valleys deepen and the overall topography becomes more pronounced, surface roughening occurs preferentially in the lower regions. Together, these findings confirm a consistent erosive mechanism driven by HCl exposure, where the retained peak acts as a real reference while surrounding areas undergo progressive dissolution.

Moreover, the progressive slight shift of the median value confirmed that the effect is not limited to isolated pits but reflects a global transformation of the surface landscape, likely corresponding to material removal at the polymer–acid interface. Importantly, no statistically significant changes were ever detected in the median levels, which strengthens the conclusion that AFM zero-level drift is negligible, and the roughening is physical and unidirectional.

Linear regressions performed on Maximum, Median, and Minimum values supported that the observed nanostructural morphological changes are unlikely to be random and are strongly correlated with immersion time in HCl solution over time, statistically significant only for the Maximum parameter (Figure 1). Accordingly, AFM trends are interpreted as within-specimen time trends.

The AFM time-lapse photos illustrated the dynamic changes, visually representing residual material's progressive acid-induced degradation and stability. Figure 2A–M shows the observed topographical changes in the DPA sample subjected to HCl at 6 min each, highlighting the increasing prominence of residual peaks as the surrounding polymer matrix progressively dissolves. Specifically, Figure 2N represents the changes in surface between timepoints, highlighted to visually detect the material etched by HCl exposure.

3.2 | ICP-MS for Elemental Release Analysis

The chemical analysis of TFAs highlighted the content of different metals in their polymeric matrix. The predominant element was tin (Sn), followed by potassium (K) and sodium (Na) with concentrations measured at 33.42 mg/kg, 21.35 mg/kg, and 13.34 mg/kg, respectively. In contrast, DPAs showed higher amounts of calcium (Ca), Na, and iron (Fe) with concentrations of 36.63 mg/kg, 11.87 mg/kg, and 32 mg/kg, respectively. The biggest difference in concentration between TFA and DPA samples was reached by Sn (31.64 mg/kg), while the smallest was by copper (Cu; 0.03 mg/kg). All these differences underscore the two aligner types' distinct compositions and leaching pathways when exposed to acidic behavior. Specific concentrations as well as RSDs and LODs are reported in Table 3.

The concentrations of metals leached after 1 week of extraction in 0.5 M HCl are presented in Table 4. The results showed trends consistent with those observed in the total metal content analysis, reflecting the chemical composition of the two aligner types. It is observable, for example, that the most abundantly leached metals are Na, Ca, K, and Fe, remarking the more concentrated metals in both TFA and DPA. One important exception is instead Sn in the TFA sample: this is the most abundant element in TFA after the acid digestion, but the leached concentration in HCl is instead lower than most of the other analyzed elements. This may be due to the chemical properties of Sn compounds added in polymers as organometals, which are less likely to be leached out in a polar solvent such as water solutions [18]. In addition, Sn may be added as a functional catalyst during the polymerization process of the resins used for these aligners, making this element potentially more strongly bonded in the crystalline polymer phase [19].

4 | Discussion

The present study aimed to investigate the transformation of plastics used for TFAs and DPAs once they reach a simulated acidic gastric environment after their mechanical fragmentation into MPs and subsequent ingestion. The analysis focused on their structural surface roughening and the leaching of elemental components.

Surface topography analysis revealed distinct roughening patterns between the materials. TFAs underwent rapid amorphization, losing their nanoscale structure and becoming unsuitable for detailed atomic force AFM imaging. Under gastric acid, ester linkages in the copolyester of TFA are rapidly hydrolyzed, and additives/lamination adhesives can leach, promoting swelling and loss of cohesion. Probably because the laminate's acid-labile core controls bulk behavior, TFA rapidly softened into an amorphous mass and could not be AFM-tracked. Supporting this structural change, a prior in vitro study in oral environments simulating acidic pH highlighted changes regarding the physical properties of TFAs [4]. Moreover, cleaners characterized by

TABLE 2 | Surface data from AFM of DPA sample, analyzed at the baseline (T0) and after 1 h of HCl exposure (T10). *P*-values refer to linear regression significance testing changes over time.

Parameter	T0 (0 min)	T1 (6min)	T2 (12min)	T3 (18min)	T4 (24min)	T5 (30min)	T6 (36min)	T7 (42min)	T8 (48min)	T9 (54min)	T10 (1 h)	*p*
Average value (nm)	0.07	0.08	0.08	0.08	0.08	0.09	0.08	0.09	0.09	0.09	0.09	0.101
RMS roughness (Sq) (nm)	10.06	10.06	10.25	10.39	10.18	10.57	10.28	10.47	10.68	10.95	10.97	< 0.001
Mean roughness (Sa) (nm)	7.85	7.93	8.11	8.23	7.97	8.31	7.93	8.13	8.22	8.56	8.49	0.002
Excess kurtosis	0.64	0.36	0.37	0.07	0.64	0.15	0.68	0.37	0.56	0.11	0.62	0.661
Maximum (nm)	42.40	40.64	36.99	35.37	38.92	36.87	38.71	36.93	46.12	42.32	51.78	0.022
Median (nm)	−1.63	−1.69	−2.04	−1.25	−1.94	−1.21	−2.07	−1.62	−1.62	−1.28	−1.86	0.960
Minimum (nm)	−25.91	−28.09	−26.27	−27.06	−24.06	−25.74	−25.66	−25.68	−23.73	−28.05	−24.73	0.284
Maximum peak height (Sp) (nm)	42.33	40.55	36.91	35.29	38.88	36.77	38.62	36.84	46.03	42.24	51.69	0.022
Maximum pit depth (Sv) (nm)	25.98	28.18	26.36	27.14	24.15	25.84	25.74	25.76	23.82	28.58	24.82	0.286
Maximum Height (Sz) (nm)	68.31	68.73	63.27	62.43	63.03	62.61	64.37	62.60	69.85	70.82	76.51	0.038

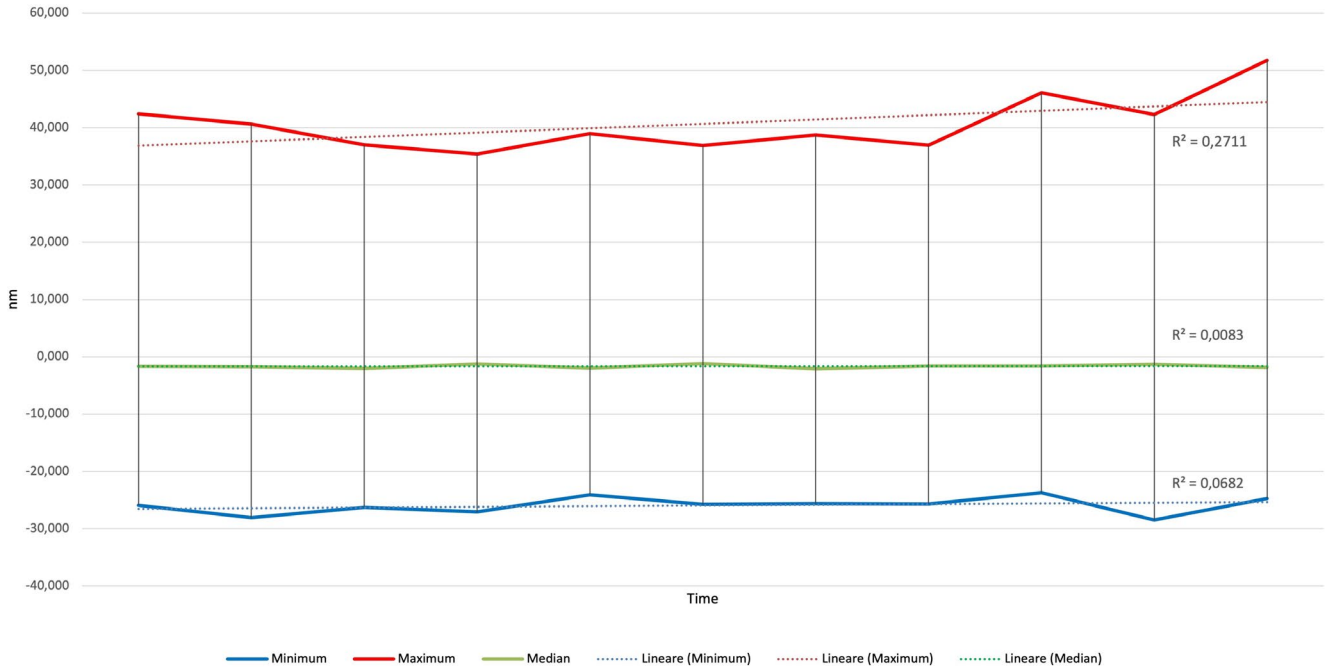

FIGURE 1 | Linear regression lines of maximum, median, and minimum values between T0 (baseline).

different pH levels have been related to surface chemical composition changes [20]; the authors reported alteration of polyester and polyurethane materials, i.e., Invisalign one, when they are subjected to the alkaline solutions only.

In contrast, crosslinked urethane-(meth)acrylate of DPA resin displayed progressive surface erosion, with nanoscale features persisting over time; its network resisted short-term bulk dissolution, so it was observed surface roughening without macroscopic disintegration. This controlled degradation could influence how DPA-derived MPs might interact with gastric mucosa, particularly regarding adhesion, transport, and potential uptake by epithelial cells. Unfortunately, no previous studies have been carried out about this aspect, limiting the comparison of the present results with other investigations.

Although the present pH-only model was designed to isolate acid-driven effects, the physiological gastric environment also contains enzymes that may act synergistically with acid, notably pepsin. Invisalign SmartTrack is a proprietary multilayer aromatic thermoplastic polyurethane with a co-polyester core [21], while Graphy TC-85DAC is a UV-cured, crosslinked aliphatic urethane-acrylate resin containing photoinitiators, per its safety data sheet. Under gastric pH, ester-containing domains in both copolyester and urethane-acrylate networks are vulnerable to acid-catalyzed hydrolysis, whereas ether-rich thermoplastic polyurethane segments are relatively more hydrolysis-resistant [22, 23]. Importantly, pepsin does not cleave these polymers directly but rapidly adsorbs to plastic surfaces to form a protein "corona" that alters charge and wettability, promotes aggregation, and can retain protons at the interface, thereby potentiating acid-driven scission and surface roughening [24]. Evidence for this enzyme–acid synergy includes pepsin-containing gastric fluids forming coronas on plastics and shifting their aggregation potential, as well as digestion-associated coronas persisting and modifying particle behavior. Therefore, in vivo pepsin is expected to adsorb and form a protein corona that retains protons at the interface, further potentiating acid-driven hydrolysis, likely accelerating TFA degradation even more than in the present in vitro pH-only model. Besides pepsin, gastric lipase and mucin may alter or amplify acid-catalyzed hydrolysis; also, gastric electrolytes (NaCl/KCl) and dietary acids/co-solvents (e.g., acetic/citric acid, ethanol) can further increase additive migration and surface damage under gastric conditions. Therefore, enzyme-supplemented tests should quantify gastric factor-mediated interfacial effects on these chemistries [25].

Chemical elemental analysis further differentiated the two materials. TFA leachates contained detectable tin and antimony, consistent with residual catalyst species reported for certain thermoplastic polyester/polyurethane formulations [19]. By contrast, DPA leachates showed titanium and chromium at low levels, plausibly originating from pigments/fillers or trace impurities typical of urethane-methacrylate photopolymers. These results indicate that the gastric-phase behavior of aligner-derived MPs is strongly material-dependent. For TFAs, the detection of Sb and Sn merits caution, noting that risk depends on dose and speciation rather than total element alone. For DPAs, Ti and Cr are often present as stable oxides or trivalent species, yet their bioaccessibility after gastric processing and downstream intestinal fate remains to be defined. In enzyme-supplemented gastric fluids (e.g., pepsin), protein coronas may further modulate interfacial leaching; therefore, elemental leachate fingerprints, rather than bulk composition alone, may be a practical strategy to trace aligner-derived MPs in biological and environmental samples.

Finally, it should be clear that the effect of released MPs and NPs on human health is not yet fully understood, but improved

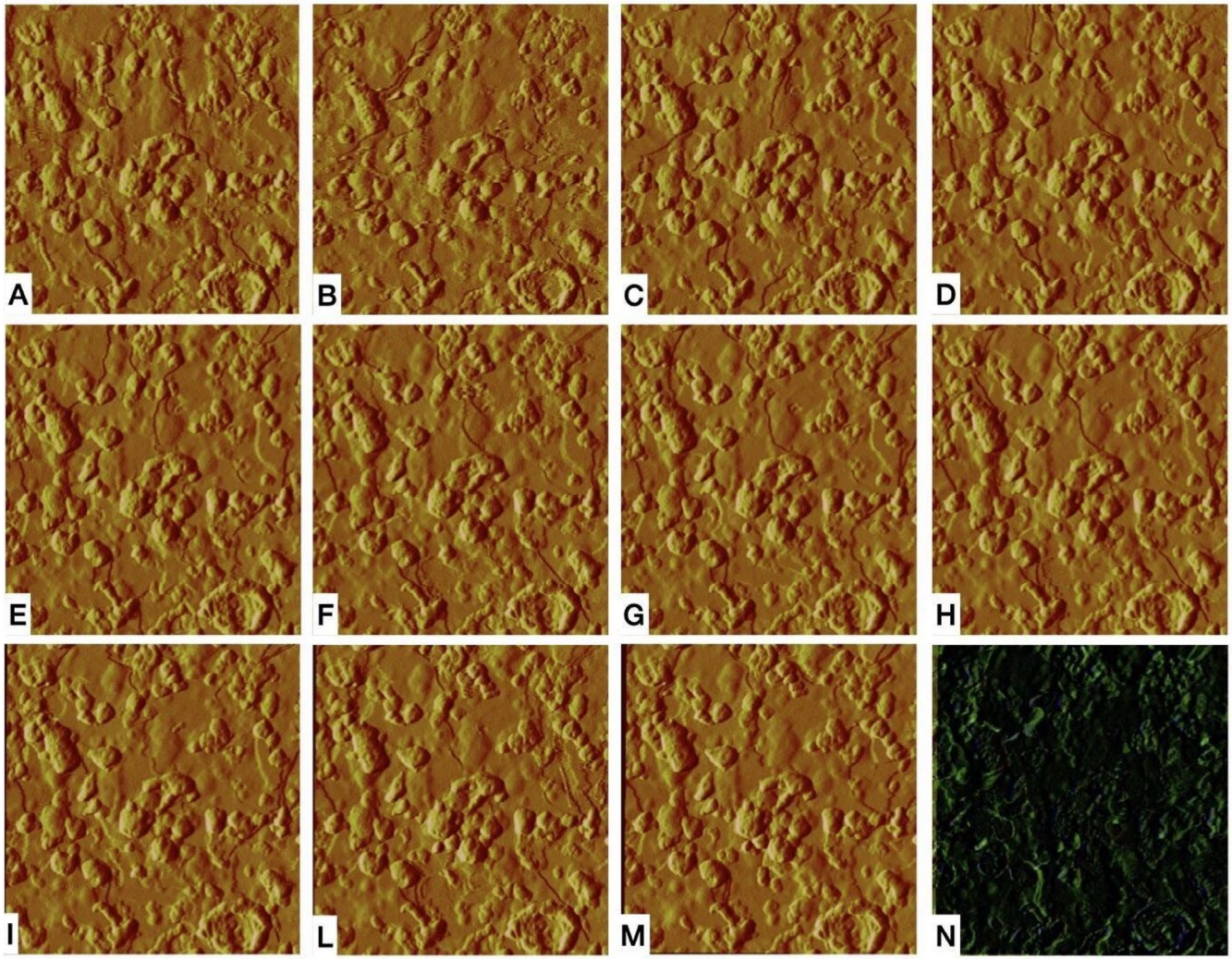

FIGURE 2 | (A–M) represents AFM scans of the 3D direct printed aligner sample on a 1 × 1 μm field at 6 min intervals; Figure 2N shows the differences between the first and the last frame; green area highlights the corroded material.

quality control during medical device manufacturing could help reduce the related risks during their use [26]. As a matter of fact, under gastric conditions, aligner-derived MPs/NPs are expected to acquire a digestion-associated protein corona and undergo acid-driven interfacial changes that can alter bioactivity and leaching. Recent in vitro studies show higher biological engagement after gastric processing, also promoted by pepsin-rich gastric fluids [27, 28]. Fortunately, aligner-specific literature further notes chemical leaching and variable cytotoxicity for 3D-printed resins depending on formulation and post-curing, underscoring product-specific risk profiles [29, 30]. With respect to human health, gastrointestinal-model studies report epithelial uptake/translocation of plastic particles and barrier/oxidative-stress responses, which plausibly intensify when particles arrive preconditioned by gastric digestion [31, 32]. Therefore, ensuring material safety should remain a priority for future aligners, as near-continuous wear for months to years leads to repeated ingestion of wear debris and associated elements, making cumulative exposure a plausible concern.

5 | Limitations

While the study provides relevant data, it also presents several limitations. The simulated gastric environment does not fully replicate the complexity of physiological conditions, such as enzymatic activity, motility, and temperature variability. In fact, the present in vitro model lacked gastric enzymes and peristaltic shear; both could interact with acid to accelerate surface roughening and leachate formation. Moreover, the analysis was limited to the external surface of the aligners, and the observation was conducted on one DPA specimen; between-specimen variability was not estimated.

Additionally, the chemical analysis focused on identifying individual elements released during exposure without considering the possible formation of secondary compounds.

Finally, because polymer composition, laminate design, cross-link density, catalysts/photoinitiators, and post-curing vary across commercial products, the present head-to-head results

TABLE 3 | Average metal concentration after acid digestion of the aligners in mg/kg. The precision of the measurements (RSD) and the detection limits (LOD) of the different elements analyzed for both TFA and DPA samples are also reported.

		TFA		DPA	
Component	**LOD (mg/kg)**	**Concentration (mg/kg)**	**RSD (%)**	**Concentration (mg/kg)**	**RSD (%)**
Na	2	13.34	2.44	11.87	5.47
Mg	0.21	<LOD	—	0.26	13.49
Al	1.2	5.55	24.72	1.87	17.64
K	1.5	21.35	20.7	1.78	14.43
Ca	7.5	8.89	11.42	36.63	14.7
Ti	0.039	0.07	26.04	0.57	30.67
Cr	0.018	0.02	29.14	0.76	26.6
Mn	0.03	0.05	35.25	0.17	34.5
Fe	2.6	4.97	11.86	3.20	13.65
Cu	0.08	0.19	8.69	0.22	9.2
Sr	0.022	0.04	16.97	0.12	14.97
Sn	0.007	33.42	1.57	1.78	15.56
Sb	0.007	0.27	3.21	0.07	32.33

TABLE 4 | Average metal concentration from the different aligners after 1 week of 0.5 M HCl extraction (expressed in mg/kg of the aligner mass). The precision of the measurements (RSD) and the detection limits (LOD) of the different elements analyzed for both TFA and DPA samples are also reported.

		TFA		DPA	
Component	**LOD (mg/kg)**	**Concentration (mg/kg)**	**RSD (%)**	**Concentration (mg/kg)**	**RSD (%)**
Na	6.01	8.62	0.23	6.89	5.07
Mg	0.08	<LOD	—	<LOD	—
Al	0.4	0.65	2.02	1.07	11.79
K	0.14	9.53	1.7	0.28	13.69
Ca	2.9	4.06	9.29	7.57	1.37
Ti	0.007	0.04	1.96	0.04	8.43
Cr	0.05	<LOD	3.99	0.05	31.42
Mn	0.004	0.02	23.51	0.03	15.27
Fe	0.19	0.73	0.12	1.57	14.03
Cu	0.02	0.08	0.59	0.04	14.38
Sr	0.004	0.008	15.45	0.01	11.47
Sn	0.005	0.09	1.01	0.11	3.55
Sb	0.005	0.13	1.49	0.03	6.3

should be interpreted as product-specific rather than category-wide; future studies should include more of these materials to evaluate whether different brands of TFA and DPA exhibit the same chemical behavior.

6 | Conclusion

The results of the present study highlighted key differences between the materials studied. TFA material (Invisalign SmartTrack)

proved to be more macroscopically vulnerable to corrosion in an acidic environment, undergoing a rapid degradation of the surface structure that made AFM analysis impossible due to the formation of an amorphous, undefined mass. In contrast, DPA material (Graphy TC-85DAC) maintained greater microscopic surface integrity, resulting in better resistance to acidic-induced degradation.

Spectroscopic analysis of the residues revealed differences in the ionic composition of the materials released during acid exposure. These results suggested that 3D-printable resins, despite some limitations, represent a more stable option and resist acidic pH.

Furthermore, this manuscript demonstrates that orthodontic aligners use plastics that exhibit a different chemical behavior upon reaching the stomach when ingested MPs and NPs produced by mechanical stress during oral wearing. These conclusions apply only to the materials tested and warrant confirmation across additional thermoformed and 3D-printed formulations.

Acknowledgments

Scientific support from the CRIETT center of the University of Insubria (instrument codes MIC02 and MAC10) is greatly acknowledged. Open access publishing facilitated by Universita degli Studi di Milano, as part of the Wiley - CRUI-CARE agreement.

Conflicts of Interest

The authors declare no conflicts of interest.

Data Availability Statement

The data that support the findings of this study is available from the corresponding author upon reasonable request.

References

1. T. Torkomian, F. de la Iglesia, and A. Puigdollers, "3D-Printed Clear Aligners: An Emerging Alternative to the Conventional Thermoformed Aligners? – A Systematic Review," *Journal of Dentistry* 155 (2025): 105616, https://doi.org/10.1016/j.jdent.2025.105616.

2. P. A. Zecca, M. Borgese, M. Raspanti, et al., "Comparative Microscopic Analysis of Plastic Dispersion From 3D-Printed and Thermoformed Orthodontic Aligners," *European Journal of Orthodontics* 47 (2025): cjaf014, https://doi.org/10.1093/ejo/cjaf014.

3. V. Quinzi, G. Orilisi, F. Vitiello, V. Notarstefano, G. Marzo, and G. Orsini, "A Spectroscopic Study on Orthodontic Aligners: First Evidence of Secondary Microplastic Detachment After Seven Days of Artificial Saliva Exposure," *Science of the Total Environment* 866 (2023): 161356, https://doi.org/10.1016/j.scitotenv.2022.161356.

4. H. M. Alkawari, L. F. Baidas, A. A. Alyahya, R. A. Alotaibi, and E. I. Alshayea, "Impact of Simulated Gastric Acid on the Physical and Mechanical Properties of Vacuum-Formed Retainers: An in Vitro Study," *BMC Oral Health* 25 (2025): 172, https://doi.org/10.1186/s12903-025-05548-8.

5. N. Koenig, J. Y. Choi, J. McCray, A. Hayes, P. Schneider, and K. B. Kim, "Comparison of Dimensional Accuracy Between Direct-Printed and Thermoformed Aligners," *Korean Journal of Orthodontics* 52 (2022): 249–257, https://doi.org/10.4041/KJOD21.269.

6. L. Šimunović, A. Jurela, K. Sudarević, I. Bačić, T. Haramina, and S. Meštrović, "Influence of Post-Processing on the Degree of Conversion and Mechanical Properties of 3D-Printed Polyurethane Aligners," *Polymers* 16 (2023): 17, https://doi.org/10.3390/polym16010017.

7. G. Iodice, B. Ludwig, E. Polishchuk, et al., "Effect of Post-Printing Curing Time on Cytotoxicity of Direct Printed Aligners: A Pilot Study," *Orthodontics & Craniofacial Research* 27 (2024): 141–146, https://doi.org/10.1111/ocr.12819.

8. F. Gamberoni, M. Borgese, C. Pagiatakis, et al., "Iron Oxide Nanoparticles With and Without Cobalt Functionalization Provoke Changes in the Transcription Profile via Epigenetic Modulation of Enhancer Activity," *Nano Letters* 23 (2023): 9151–9159, https://doi.org/10.1021/acs.nanolett.3c01967.

9. N. Panayi, S. N. Papageorgiou, G. Eliades, and T. Eliades, "Microplastics and Orthodontic Aligners: The Concerns Arising From the Modernization of Practice Through Polymers and Plastics," *Journal of the World Federation of Orthodontists* 13 (2024): 259–264, https://doi.org/10.1016/j.ejwf.2024.10.001.

10. C. Barile, C. Cianci, V. Paramsamy Kannan, et al., "Experimental Assessment of Damage and Microplastic Release During Cyclic Loading of Clear Aligners," *PLoS One* 20 (2025): e0318207, https://doi.org/10.1371/journal.pone.0318207.

11. G. Arcidiacono, E. Armentani, D. Castagnetti, et al., "Study of Damage and Microplastic Release in Clear Aligners Under Cyclic Loads," *Engineering Proceedings* 85 (2025): 16, https://doi.org/10.3390/engproc2025085016.

12. E. Fournier, L. Etienne-Mesmin, C. Grootaert, et al., "Microplastics in the Human Digestive Environment: A Focus on the Potential and Challenges Facing In Vitro Gut Model Development," *Journal of Hazardous Materials* 415 (2021): 125632, https://doi.org/10.1016/j.jhazmat.2021.125632.

13. R. Peters, N. de Jong, L. Haan, S. Wright, and H. Bouwmeester, "Release and Intestinal Translocation of Chemicals Associated With Microplastics in an In Vitro Human Gastrointestinal Digestion Model," *Microplastics and Nanoplastics* 2 (2022): 3, https://doi.org/10.1186/s43591-021-00022-y.

14. D. M. Mudie, G. L. Amidon, and G. E. Amidon, "Physiological Parameters for Oral Delivery and In Vitro Testing," *Molecular Pharmaceutics* 7 (2010): 1388–1405, https://doi.org/10.1021/mp100149j.

15. S. Carnati, A. Pozzi, D. Spanu, et al., "Towards Harmonization of Metal(Loid)s Determination in Conventional and Compostable Plastics: Comparison of Acid Digestion Protocols in LDPE and PBAT/TPS Blends," *Chemosphere* 367 (2024): 143581, https://doi.org/10.1016/j.chemosphere.2024.143581.

16. L. Sørensen, C. Zammite, A. Igartua, et al., "Towards Realism in Hazard Assessment of Plastic and Rubber Leachates – Methodological Considerations," *Journal of Hazardous Materials* 480 (2024): 136383, https://doi.org/10.1016/j.jhazmat.2024.136383.

17. E. S. Rødland, G. Binda, D. Spanu, S. Carnati, L. R. Bjerke, and L. Nizzetto, "Are Eco-Friendly Green Tires Also Chemically Green? Comparing Metals, Rubbers and Selected Organic Compounds in Green and Conventional Tires," *Journal of Hazardous Materials* 476 (2024): 135042, https://doi.org/10.1016/j.jhazmat.2024.135042.

18. A. Turner and M. Filella, "Hazardous Metal Additives in Plastics and Their Environmental Impacts," *Environment International* 156 (2021): 106622, https://doi.org/10.1016/j.envint.2021.106622.

19. G. Binda, S. Carnati, N. Passignani, et al., "A Screening of Metal(Loid) Content in Conventional and Compostable Plastic Polymers: Understanding the Sources and the Connected Environmental Implications," *Environmental Pollution* 375 (2025): 126364, https://doi.org/10.1016/j.envpol.2025.126364.

20. A. Iliadi, V. Enzler, G. Polychronis, T. Peltomaki, S. Zinelis, and T. Eliades, "Effect of Cleansers on the Composition and Mechanical Properties of Orthodontic Aligners In Vitro," *Progress in Orthodontics* 23 (2022): 54, https://doi.org/10.1186/s40510-022-00449-w.

21. L. Memè, V. Notarstefano, F. Sampalmieri, G. Orilisi, and V. Quinzi, "ATR-FTIR Analysis of Orthodontic Invisalign Aligners Subjected to

Various In Vitro Aging Treatments," *Materials* 14 (2021): 818, https://doi.org/10.3390/ma14040818.

22. D. V. Orekhov, O. A. Kazantsev, A. P. Sivokhin, and M. V. Savinova, "Features of the Acid-Catalyzed Hydrolysis of Mono- and Poly(Ethylene Glycol) Methacrylates," *European Polymer Journal* 100 (2018): 18–24, https://doi.org/10.1016/j.eurpolymj.2018.01.010.

23. L. M. Gradinaru, F. Doroftei, and S. Vlad, "Insights Into the Stability of Poly(Ether Urethane) Composite Membranes Containing Magnetic Nanoparticles," *Colloids and Surfaces A: Physicochemical and Engineering Aspects* 686 (2024): 133466, https://doi.org/10.1016/j.colsurfa.2024.133466.

24. H. Brouwer, M. Porbahaie, S. Boeren, M. Busch, and H. Bouwmeester, "The In Vitro Gastrointestinal Digestion-Associated Protein Corona of Polystyrene Nano- and Microplastics Increases Their Uptake by Human THP-1-Derived Macrophages," *Particle and Fibre Toxicology* 21 (2024): 4, https://doi.org/10.1186/s12989-024-00563-z.

25. A. Brodkorb, L. Egger, M. Alminger, et al., "INFOGEST Static In Vitro Simulation of Gastrointestinal Food Digestion," *Nature Protocols* 14 (2019): 991–1014, https://doi.org/10.1038/s41596-018-0119-1.

26. B. L. M. Fontes, L. C. d. S. e. Souza, A. P. S. da Silva de Oliveira, R. N. da Fonseca, M. P. C. Neto, and C. R. Pinheiro, "The Possible Impacts of Nano and Microplastics on Human Health: Lessons From Experimental Models Across Multiple Organs," *Journal of Toxicology and Environmental Health. Part B, Critical Reviews* 27 (2024): 153–187, https://doi.org/10.1080/10937404.2024.2330962.

27. Z. Shao, J. Su, J. Dong, et al., "Aggregation Kinetics of Polystyrene Nanoplastics in Gastric Environments: Effects of Plastic Properties, Solution Conditions, and Gastric Constituents," *Environment International* 170 (2022): 107628, https://doi.org/10.1016/j.envint.2022.107628.

28. X. j. Chen, J. j. Ma, R. l. Yu, G. r. Hu, and Y. Yan, "Bioaccessibility of Microplastic-Associated Heavy Metals Using an In Vitro Digestion Model and Its Implications for Human Health Risk Assessment," *Environmental Science and Pollution Research* 29 (2022): 76983–76991, https://doi.org/10.1007/s11356-022-20983-8.

29. M. Lorusso, F. Esperouz, G. Di Carlo, et al., "Cytotoxicity of Printed Aligners: A Systematic Review," *Dentistry Journal* 13, no. 7 (2025): 275, https://doi.org/10.3390/dj13070275.

30. M. Ferreira, H. Costa, N. Veiga, M. J. Correia, A. T. P. C. Gomes, and P. C. Lopes, "Do Clear Aligners Release Toxic Chemicals?—A Systematic Review," *Journal of Functional Biomaterials* 16 (2025): 173, https://doi.org/10.3390/jfb16050173.

31. R. Jia, J. Han, X. Liu, et al., "Exposure to Polypropylene Microplastics via Oral Ingestion Induces Colonic Apoptosis and Intestinal Barrier Damage Through Oxidative Stress and Inflammation in Mice," *Toxics* 11 (2023): 127, https://doi.org/10.3390/toxics11020127.

32. G. M. DeLoid, X. Cao, D. Bitounis, et al., "Toxicity, Uptake, and Nuclear Translocation of Ingested Micro-Nanoplastics in an In Vitro Model of the Small Intestinal Epithelium," *Food and Chemical Toxicology* 158 (2021): 112609, https://doi.org/10.1016/j.fct.2021.112609.